The Journal of Physical Chemistry B

 VOLUME 103, NUMBER 33, AUGUST 19, 1999

LETTERS

Primary Process of Photocarrier Generation in Y-Form Titanyl Phthalocyanine Studied by Electric-Field-Modulated Picosecond Time-Resolved Fluorescence Spectroscopy

Shoichi Yamaguchi* and Yutaka Sasaki

Yokohama Research Center, Mitsubishi Chemical Corporation, 1000 Kamoshida, Aoba, Yokohama 227-8502, Japan

Received: June 9, 1999

We have investigated the primary process of the carrier generation in Y-form titanyl phthalocyanine (Y-TiOPc) microcrystallites by means of newly developed electric-field-modulated picosecond time-resolved fluorescence spectroscopy. Two singlet excitons have been identified in the fluorescence decay curves of Y-TiOPc. We have inferred from the field-dependence of the fluorescence amplitudes and lifetimes that the shorter-lifetime exciton of intramolecular charge transfer (CT) character is a primary intermediate in the carrier generation process. It has been found that the internal conversion from the CT exciton to the Frenkel exciton is decelerated by the electric field.

I. Introduction

Phthalocyanines (Pcs) are known as highly photoconductive materials. They exhibit very strong absorption in the near-infrared (NIR) and visible (vis) region, and the photoexcitation brings about free carrier generation with quite high quantum yield. The strong NIR absorption band called "Q band" makes Pcs one of the best carrier-generation materials (CGM) of digital electrophotography. The carrier-generation process is roughly depicted as follows: NIR or vis photoexcitation generates a singlet exciton which partly decays to a geminate bound electron−hole pair. The bound pair subsequently dissociates into free carriers with the aid of an external electric field. The latter dissociation process is well described by the Onsager theory[1] or the Noolandi−Hong model.[2] However, the former primary process has not yet been well understood despite its importance to the carrier quantum yield. At least we have to know the decay pathways of a singlet exciton which are still beyond theoretical or computational treatment at the present stage.

The photoconductive properties of Pcs depends on polymorphs as well as central metals. Electrophotographic data reviewed by Law[3] have showed that titanyl phthalocyanine of the Y-polymorph (Y-TiOPc) has the best photoconductivity among H_2Pcs, CuPcs, VOPc, AlClPc, TiOPcs of the other polymorphs, and so on. The photocarrier-generation quantum yield of Y-TiOPc has been estimated at more than 0.9.[3] The carrier-generation mechanism of Y-TiOPc has been discussed by many researchers.[4−9] Popovic et al.[9] reported the electric-field-induced quenching of steady-state and time-resolved fluorescence in Y-TiOPc. Electric-field application generally increases the quantum yield of the carrier generation, and subsequently decreases that of fluorescence. They found two components of different lifetimes in their fluorescence decay curves. They observed electric-field-induced amplitude quenching and lifetime shortening as regards both of these two transient components. They assigned the shorter-lifetime component to a charge-transfer (CT) exciton and regarded it as a carrier precursor.

In the present Letter, we give a new explanation for the primary carrier-generation process of Y-TiOPc on the basis of

* Author to whom correspondence should be addressed. Telephone: +81-45-963-3155. Fax: +81-45-963-3974. E-mail: picco@rc.m-kagaku.co.jp.

10.1021/jp991892w CCC: $18.00
Published on Web 08/04/1999

electric-field-modulated picosecond time-resolved fluorescence spectroscopic data.

II. Experimental Section

Thin-film sandwich cells on NESA glass substrates were used as samples. On NESA, alcohol-soluble nylon was first spin-coated as a blocking layer of 1.6 μm. A 0.5 μm Y-TiOPc layer was then spin-coated. The Y-TiOPc pigment was dispersed in poly(vinylbutyral) solution. Third, a polycarbonate blocking layer of 0.6 μm was spin-coated on the pigment layer. Finally, aluminum was evaporated over the polycarbonate layer to form an electrode. The diameter of the Y-TiOPc microcrystallites was about 0.1 μm.

Picosecond time-resolved fluorescence spectra were measured by using a streak scope (HAMAMATSU, C4334) with an imaging spectrograph (CHROMEX, 250is). The streak scope was driven in a photon-counting mode. The fluorescence excitation source was provided by a mode-locked Ti:Sapphire laser (Coherent, MIRA900) at a repetition rate of 75.5 MHz. The time-resolution was about 15 ps that was limited by the streak scope. The excitation wavelength was 800 nm. The excitation density was 0.3 mW mm^{-2} (average power) or 4 pJ mm^{-2} (pulse energy). It took about 5 min to obtain one streak image.

The electric-field-modulated picosecond time-resolved fluorescence spectrometer was newly developed by utilizing a special chopper in addition with the same picosecond fluorescence measurement system as above. The excitation laser beam was divided into two by a beam splitter. One beam was chopped by the outer part of the chopper blade, and the other was chopped by the inner part. The chopper blade blocked these two beams alternately at about 30 Hz. The two beams were again made to be collinear by a beam splitter, and illuminated the sample. The optical path length of one beam between the first beam splitter and the second one was set to be about 30 cm ($\sim$1 ns) longer than that of the other beam. Square-wave electric bias synchronized with the chopper was applied to the sample. Consequently, the sample was illuminated by one beam when the applied electric field was on, and by the other beam when the electric field was off. Let us call the former beam "on beam", and the latter "off beam". The sweep range of the streak scope was set to 2 ns. The fluorescence that originated from the "on beam" formed a streak image in the spatially upper part of the CCD of the streak scope that corresponds to a temporally earlier area (0$-$1 ns), and that from the "off beam" formed another image in the spatially lower part that corresponds to temporally later one (1$-$2 ns). There was almost no overlap between these two images, because the fluorescence lifetimes were much shorter than 1 ns that was the path-length difference between the two beams. The two images were put in the sweep time of 2 ns, and the time resolution of 15 ps was enough to obtain the fluorescence lifetimes. The streak image in the upper part included electric-field-modulated signals, and that in the lower part served as an internal standard. Thanks to the internal standard, we could cancel out the contribution of laser-intensity fluctuation and streak-scope trigger-timing jitter, and succeeded in obtaining an electric-field-induced change of a lifetime and that of an amplitude as small as 1% without losing the two-dimension advantage of the streak scope.

III. Results and Discussion

The streak images of the Y-TiOPc samples were analyzed by fitting the temporal profiles of the fluorescence intensity at each wavelength to a simple model function. The model function

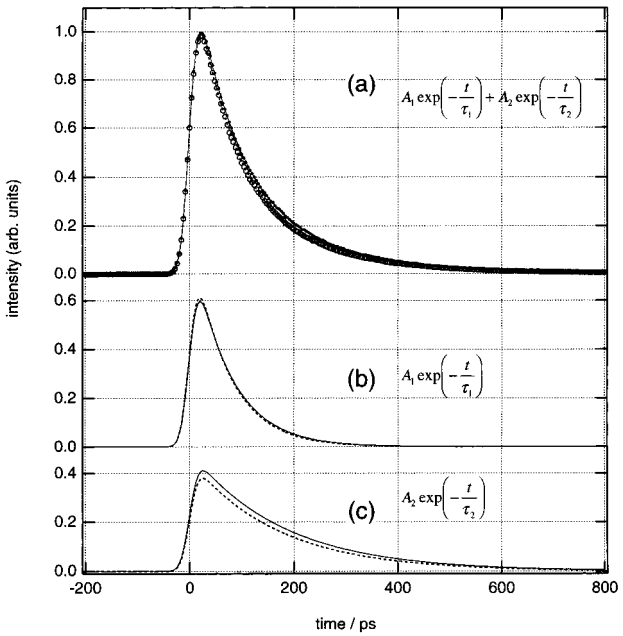

Figure 1. (a) Fluorescence decay curves of Y-TiOPc at 870 $\pm$ 20 nm under no electric field (small solid circles: data, line: fitting) and under 30-V μm^{-1} electric field (large open circles: data, broken line: fitting). (b) Shorter-lifetime fitting component (line: no electric field, broken line: 30 V μm^{-1}). (c) Longer-lifetime fitting component (line: no electric field, broken line: 30 V μm^{-1}).

TABLE 1: Electric-Field Dependence of Fluorescence Lifetimes

	electric field	
time-const.	0 V μm^{-1}	30 V μm^{-1}
τ_1/ps	72	69
τ_2/ps	175	166

TABLE 2: Electric-Field Dependence of Fluorescence Amplitudes and Integrated Total Intensity

x	$\frac{\text{x(30 V } \mu\text{m}^{-1})}{\text{x(0 V } \mu\text{m}^{-1})}$
A_1	1.02
A_2	0.92
$A_1 + A_2$	0.99
$A_1\tau_1 + A_2\tau_2$	0.93

was the convolution of an instrumental response and a sum of two exponentials expressed as

$$A_1 \exp\left(-\frac{t}{\tau_1}\right) + A_2 \exp\left(-\frac{t}{\tau_2}\right) \quad (1)$$

The amplitudes (A_1, A_2) and the time constants (τ_1, τ_2) were treated as fitting parameters. All the fitting procedures converged successfully. It was found that τ_1, τ_2, and A_1/A_2 did not depend on wavelength. Therefore we integrated the fluorescence intensity in the wavelength range 870 $\pm$ 20 nm to obtain the fluorescence decay curves with good signal-to-noise ratio. The temporal profiles were normalized by the internal standard. In Figure 1a, the fluorescence decay curves of Y-TiOPc are shown with the fitting results. The two fitting components, $A_1 \exp(-t/\tau_1)$ and $A_2 \exp(-t/\tau_2)$, are separately shown in Figure 1, parts b and c, respectively. The obtained fitting parameters are summarized in Tables 1 and 2. The decay curve under the electric field of 30 V μm^{-1} slightly deviates from that under no electric field in Figure 1a. This deviation is due mainly to

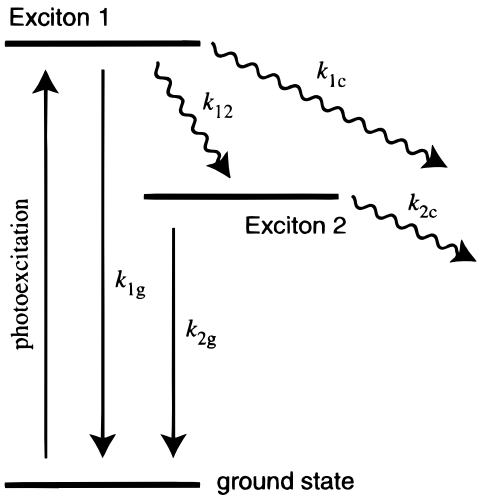

Figure 2. Schematic diagram of the primary process after photoexcitation in Y-TiOPc. Straight arrows stand for radiative transitions, and wavy arrows represent nonradiative relaxation process.

the longer-lifetime component as can be seen in Figure 1c. We can see in Table 1 that the electric field reduces the lifetimes of both of the two components. While the electric-field-induced amplitude quenching of the longer-lifetime component (A_2) is clearly confirmed in Table 2, A_1 slightly increases upon the electric-field application. The temporally integrated total fluorescence intensity which is proportional to $A_1\tau_1 + A_2\tau_2$ decreased by 7% upon the electric-field application.

The successful fitting to the simple model function means that there are two singlet excitons, both of which show monomeric decays. The most tenable diagram of the exciton dynamics is schematically shown in Figure 2. Exciton 1 corresponds to the shorter-lifetime component. The decay rate of exciton 1 (τ_1^{-1}) is the sum of the radiative decay rate (k_{1g}), the internal conversion rate (k_{12}), and the rate of the other decay (k_{1c}). The carrier generation pathway may be included in the other decay. Exciton 2 decays either to the ground state radiatively with a rate of k_{2g} or to the other state with a rate of k_{2c}. It is easy to write down the total fluorescence intensity $I(t)$ after photoexcitation at $t = 0$:

$$I(t) = c_1 \exp\left(-\frac{t}{\tau_1}\right) + \frac{c_2 k_{12}}{\frac{1}{\tau_1} - \frac{1}{\tau_2}}\left\{\exp\left(-\frac{t}{\tau_2}\right) - \exp\left(-\frac{t}{\tau_1}\right)\right\}, \quad (2)$$

where c_1 and c_2 are constant coefficients. The first term of rhs of eq 2 is due to exciton 1, and the second term is due to exciton 2. We obtain two important equations by comparing eq 2 with eq 1:

$$A_1 + A_2 = c_1 \quad (3)$$

$$k_{12} = c_2^{-1} A_2 \left(\frac{1}{\tau_1} - \frac{1}{\tau_2}\right) \quad (4)$$

We have already known how the electric field influences A_1, A_2, τ_1, and τ_2. Equation 3 means that the sum of A_1 and A_2 does not depend on the electric field. In fact, Table 2 shows that $A_1 + A_2$ changed little (1%) when A_2 decreased by 8% and A_1 increased by 2% upon the electric-field application. $A_1 + A_2$ corresponds to the initial population of exciton 1 prepared by the photoexcitation in the present scheme and should be independent of the electric field. We are going to check the 1% decrease of $A_1 + A_2$ soon by improving the signal-to-noise ratio.

By using eq 4, Tables 1 and 2, we can obtain a relative value of the internal conversion rate k_{12}. It is found that k_{12} decreases by 5% upon the electric-field application. In other words, the electric field decelerates the internal conversion from exciton 1 to exciton 2. The radiative decay rate k_{1g} is reasonably regarded as field-independent. Since τ_1 becomes shorter upon the electric-field application, k_{1c} surely increases. It is confirmed that the A_2 decrease as large as 8% is ascribed to both the k_{12} decrease and the k_{1c} increase. It is also affirmed that the k_{2c} increase induced by the electric field makes τ_2 shorter.

Let us consider why there are two kind of nonradiative decay pathways, one of which is accelerated by the electric field and the other is decelerated. We all know that an electric field promotes carrier generation. An electric field probably promotes charge separation not only in the Onsager process where a bound pair dissociates into free carriers but also in the primary process where an exciton decays to a bound pair. It is natural to regard a relaxation pathway accelerated by electric field as a pathway connecting with the carrier generation process. The decay process denoted by k_{1c} in Figure 2 probably corresponds to relaxation to a bound electron−hole pair because of the electric-field-induced k_{1c} increase. We conclude that exciton 1 is a primary intermediate of the carrier generation process. Since the quantum yield of exciton 2 decreases upon the electric-field application, we do not know whether the process denoted by k_{2c} that is also accelerated participates in the carrier generation or not. Popovic et al.[9] assigned the slow component (corresponds to exciton 2) to trapped excitons. They regarded the slow component as unimportant in the carrier generation process. We had better not bring the role of exciton 2 to a conclusion at the present stage.

There is no precedent for the internal conversion process decelerated by the electric field to the best of our knowledge. We give a simple explanation for it. We assume that electric-field effect on a relaxation rate is determined by CT character or permanent dipole moment of the initial and final states of the process. In the decay process from exciton 1 to a bound pair, the final state has much larger permanent dipole moment than the initial state, and therefore this process is actually accelerated by the electric field. We infer from the deceleration of the internal conversion that the CT character of exciton 1 is larger than that of exciton 2. We propose a rough idea that exciton 1 is assigned to the CT exciton and exciton 2 to the neutral Frenkel exciton. Though a "CT state" in Pcs is often used to stand for an intermolecular CT state,[5,8,10,11] exciton 1 in the present case should be regarded as an intramolecular CT state. We do not think an intermolecular CT state emits significant fluorescence. The transition dipole moment between an intermolecular CT state and the ground state is so small that its contribution is observed only by precise electroabsorption (or electroreflectance) spectroscopy.[5,10,11] An intermolecular CT state would rather be regarded as a bound electron−hole pair than a singlet exciton. We conclude that exciton 1 of the intramolecular CT character is directly generated by the photoexcitation and dissociates into a bound pair that is the precursor of free carriers. Note that vibrational excess energy brought about by the photoexcitation seems to play no role in the dissociation process from exciton 1 to a bound pair, because the exciton 1 lifetime (72 ps) is long enough for vibrational relaxation to be complete in the excited singlet manifold.[12]

Finally we make comments on two discrepancies between our results and those of Popovic et al.[9] The two time constants (τ_1, τ_2) that we obtained under no electric field, 72 and 175 ps, are not in agreement with theirs, 45 and 234 ps. There are two

possible reasons for this discrepancy. First, we cannot say that our Y-TiOPc and theirs are exactly the same. Y-TiOPc is usually characterized by its X-ray powder diffraction pattern which has only three main peaks with relatively broad bandwidths. The crystal structure of Y-TiOPc has not yet been strictly determined. In addition, the Y-form is one of metastable polymorphs. It is possible that there is a slight difference between our Y-TiOPc sample and theirs. Second, we do not think that the time resolution of their measurements was sufficient. They obtained the lifetimes by using the time-correlated single-photon counting method whose best time resolution is generally about 30 ps. We are sure that it is not easy to obtain a 45-ps time constant with this method. On the other hand, the streak scope that we used has a time resolution of 15 ps as mentioned above. There is no difficulty in measuring a 72-ps decay with the streak scope. It is generally accepted that a streak scope is the best instrument for time-resolved fluorescence spectroscopy in all respects. From a spectroscopic point of view, the fluorescence lifetimes obtained by us are more reliable than those by Popovic et al. The other discrepancy is that the fluorescence quenching efficiency in their results is about four times larger than in ours. The quenching efficiency or the field-induced decrease of the integrated total fluorescence intensity was 7%, as mentioned above in our present results. Popovic et al. reported it to be about 30% under the same electric field. We reproduced our value in electric-field-modulated steady-state (not time-resolved) fluorescence measurements not only with 800-nm excitation but also with 633-nm excitation. Popovic et al. used 590-nm excitation, but we do not think that the discrepancy is due to the difference of excitation wavelength. It is noted that we have found the quenching efficiency of x-metal-free Pc under 30 V μm^{-1} to be 5% which is in good agreement with the value reported by Popovic et al. in the same paper. It means that our experiments had no systematic error. We can attribute the discrepancy to nothing but the above-mentioned sample difference.

IV. Summary

The primary process of the Y-TiOPc photocarrier generation has been studied by electric-field-modulated picosecond time-resolved fluorescence spectroscopy. The shorter-lifetime species has been assigned to the intramolecular CT exciton. The longer-lifetime species has been identified as the neutral Frenkel exciton. We regard the CT exciton as a key intermediate in the primary process of the photocarrier generation. We have shown that the internal conversion from the CT exciton to the Frenkel exciton is decelerated by the electric field.

References and Notes

(1) Onsager, L. *J. Chem. Phys.* **1934**, *2*, 599.
(2) Noolandi, J.; Hong, K. M. *J. Chem. Phys.* **1979**, *70*, 3230.
(3) Law, K.-Y. *Chem. Rev.* **1993**, *93*, 449.
(4) Popovic, Z. D.; Hor, A. *Mol. Cryst. Liq. Cryst.* **1993**, *228*, 75.
(5) Saito, T.; Sisk, W.; Kobayashi, T.; Suzuki, S.; Iwayanagi, T. *J. Phys. Chem.* **1993**, *97*, 8026.
(6) Mizuguchi, J.; Rihs, G.; Karfunkel, H. R. *J. Phys. Chem.* **1995**, *99*, 16217.
(7) Gulbinas, V.; Jakubenas, R.; Pakalnis, S.; Undzenas, A. *Adv. Mater. Opt. Electron.* **1996**, *6*, 412.
(8) Gulbinas, V.; Jakubenas, R.; Pakalnis, S.; Undzenas, A. *J. Chem. Phys.* **1997**, *107*, 4927.
(9) Popovic, Z. D.; Khan, M. I.; Atherton, S. J.; Hor, A.-M.; Goodman, J. L. *J. Phys. Chem. B* **1998**, *102*, 657.
(10) Tokura, Y.; Koda, T.; Iyechika, Y.; Kuroda, H. *Chem. Phys. Lett.* **1983**, *102*, 174.
(11) Yamasaki, K.; Okada, O.; Inami, K.; Okada, K.; Kotani, M.; Yamada, H. *J. Phys. Chem. B* **1997**, *101*, 13.
(12) Yamaguchi, S.; Hamaguchi, H. *Chem. Phys. Lett.* **1994**, *227*, 255.